



# Analysis of the nonlinear Kerr effects in optical transmission systems that deploy optical phase conjugation

MOHAMMAD A. Z. AL-KHATEEB,<sup>1,\*</sup> MD. ASIF IQBAL,<sup>1</sup> MINGMING TAN,<sup>1</sup> ABDALLAH ALI,<sup>1</sup> MARY MCCARTHY,<sup>2</sup> PAUL HARPER,<sup>1</sup> AND ANDREW D. ELLIS<sup>1</sup>

<sup>1</sup>Aston Institute of Photonic Technologies (AIPT), Aston University, Birmingham, B4 7ET, UK

<sup>2</sup>Now with Oclaro Technologies, Long Road, Paignton, TQ4 7AU, UK

\*alkhamaz@aston.ac.uk

**Abstract:** In this work, we will derive, validate, and analyze the theoretical description of nonlinear Kerr effects resulting from various transmission systems that deploy single or multiple optical phase conjugators (OPCs). We will show that the nonlinear Kerr compensation can be achieved, with various efficiencies, in both lumped and distributed Raman transmission systems. The results show that first order distributed Raman systems are superior to the discretely amplified systems in terms of the nonlinear Kerr compensation efficiency that a mid-link OPC can achieve. Also, we will show that the multi-OPC approach will diminish the nonlinearity compensation efficiency in any system as it will act as periodic dispersion compensators.

Published by The Optical Society under the terms of the [Creative Commons Attribution 4.0 License](#). Further distribution of this work must maintain attribution to the author(s) and the published article's title, journal citation, and DOI.

**OCIS codes:** (190.4380) Nonlinear optics, four-wave mixing; (190.4223) Nonlinear wave mixing; (190.5040) Phase conjugation.

## References and links

1. A. D. Ellis, M. E. McCarthy, M. A. Z. Al Khateeb, M. Sorokina, and N. J. Doran, "Performance limits in optical communications due to fiber nonlinearity," *Adv. Opt. Photonics* **9**(3), 429–503 (2017).
2. P. Poggiolini, "The GN model of non-linear propagation in uncompensated coherent optical systems," *J. Lightwave Technol.* **30**(24), 3857–3879 (2012).
3. K. O. Hill, D. C. Johnson, B. S. Kawasaki, and R. I. MacDonald, "CW three-wave mixing in single-mode optical fibers," *J. Appl. Phys.* **49**(10), 5098–5106 (1978).
4. A. D. Ellis and W. A. Stallard, "Four wave mixing in ultra long transmission systems incorporating linear amplifiers," in *Proceedings of IEE Colloquium on Non-Linear Effects in Fibre Communications* (IEEE, 1990), 6/1–6/4.
5. D. G. Schadt, "Effect of amplifier spacing on four-wave mixing in multichannel coherent communications," *Electron. Lett.* **27**(20), 1805–1807 (1991).
6. K. Inoue, "Phase-mismatching characteristic of four-wave mixing in fiber lines with multistage optical amplifiers," *Opt. Lett.* **17**(11), 801–803 (1992).
7. D. A. Cleland, A. D. Ellis, and C. H. F. Sturrock, "Precise modelling of four wave mixing products over 400 km of step-index fibre," *Electron. Lett.* **28**(12), 1171–1173 (1992).
8. N. Shibata, R. Braun, and R. Waarts, "Phase-mismatch dependence of efficiency of wave generation through four-wave mixing in a single-mode optical fiber," *IEEE J. Quantum Electron.* **23**(7), 1205–1210 (1987).
9. C. Kurtzke, "Suppression of fiber nonlinearities by appropriate dispersion management," *IEEE Photonics Technol. Lett.* **5**(10), 1250–1253 (1993).
10. M. E. Marhic, N. Kagi, T. K. Chiang, and L. G. Kazovsky, "Optimizing the location of dispersion compensators in periodically amplified fiber links in the presence of third-order nonlinear effects," *IEEE Photonics Technol. Lett.* **8**(1), 145–147 (1996).
11. K. Nakajima, M. Ohashi, K. Shiraki, T. Horiguchi, K. Kurokawa, and Y. Miyajima, "Four-wave mixing suppression effect of dispersion distributed fibers," *J. Lightwave Technol.* **17**(10), 1814–1822 (1999).
12. K. Inoue and H. Toba, "Fiber four-wave mixing in multi-amplifier systems with nonuniform chromatic dispersion," *J. Lightwave Technol.* **13**(1), 88–93 (1995).

13. W. Zeiler, F. Di Pasquale, P. Bayvel, and J. E. Midwinter, "Modeling of four-wave mixing and gain peaking in amplified WDM optical communication systems and networks," *J. Lightwave Technol.* **14**(9), 1933–1942 (1996).
14. S. Radic, G. Pendock, A. Srivastava, P. Wysocki, and A. Chraplyvy, "Four-wave mixing in optical links using quasi-distributed optical amplifiers," *J. Lightwave Technol.* **19**(5), 636–645 (2001).
15. S. Watanabe and M. Shirasaki, "Exact compensation for both chromatic dispersion and Kerr effect in a transmission fiber using optical phase conjugation," *J. Lightwave Technol.* **14**(3), 243–248 (1996).
16. V. Pechenkin and I. J. Fair, "On four-wave mixing suppression in dispersion-managed fiber-optic OFDM systems with an optical phase conjugation module," *J. Lightwave Technol.* **29**(11), 1678–1691 (2011).
17. M. Al-Khateeb, M. E. McCarthy, and A. D. Ellis, "Experimental verification of four wave mixing in lumped optical transmission systems that employ mid-link optical phase conjugation," in *Conference on Lasers and Electro-Optics*, OSA Technical Digest (online) (Optical Society of America, 2017), paper JTh2A.64.
18. A. D. Ellis, M. E. McCarthy, M. A. Z. Al-Khateeb, and S. Sygletos, "Capacity limits of systems employing multiple optical phase conjugators," *Opt. Express* **23**(16), 20381–20393 (2015).
19. M. A. Z. Al-Khateeb, M. McCarthy, C. Sánchez, and A. Ellis, "Effect of second order signal-noise interactions in nonlinearity compensated optical transmission systems," *Opt. Lett.* **41**(8), 1849–1852 (2016).
20. M. E. McCarthy, M. A. Z. Al-Khateeb, F. M. Ferreira, and A. D. Ellis, "PMD tolerant nonlinear compensation using in-line phase conjugation," *Opt. Express* **24**(4), 3385–3392 (2016).
21. M. A. Z. Al-Khateeb, M. Tan, M. A. Iqbal, M. McCarthy, P. Harper, and A. D. Ellis, "Four wave mixing in distributed Raman amplified optical transmission systems," in *Proceedings of IEEE Photonics Conference* (IEEE, 2016), pp. 795–796.
22. W. Shieh, "Information spectral efficiency and launch power density limits due to fiber nonlinearity for coherent optical OFDM systems," *J. Photonics* **3**(2), 158–173 (2011).
23. X. Chen and W. Shieh, "Closed-form expressions for nonlinear transmission performance of densely spaced coherent optical OFDM systems," *Opt. Express* **18**(18), 19039–19054 (2010).
24. C. Headley and G. P. Agrawal, *Raman Amplification in Fiber Optical Communication Systems* (Elsevier, 2005).
25. M. Tan, P. Rosa, M. A. Iqbal, I. Phillips, J. Nuño, J. D. Ania-Castanon, and P. Harper, "RIN mitigation in second-order pumped Raman fibre laser based amplification," in *Asia Communications and Photonics Conference*, OSA Technical Digest (online) (Optical Society of America, 2015), paper AM2E.6.
26. M. H. Shoreh, "Compensation of nonlinearity impairments in coherent optical OFDM systems using multiple optical phase conjugate modules," *J. Opt. Commun. Netw.* **6**(6), 549–558 (2014).
27. P. Minzioni and A. Schiffrini, "Unifying theory of compensation techniques for intrachannel nonlinear effects," *Opt. Express* **13**(21), 8460–8468 (2005).
28. S. L. Jansen, D. Van Den Borne, B. Spinnler, S. Calabrò, H. Suche, P. M. Krummrich, W. Sohler, G. Khoe, and H. De Waardt, "Optical phase conjugation for ultra long-haul a phase-shift-keyed transmission," *J. Lightwave Technol.* **24**(1), 54–64 (2006).
29. P. Minzioni, "Nonlinearity compensation in a fiber optic link by optical phase conjugation," *Fiber Integr. Opt.* **28**, 179–209 (2009).

## 1. Introduction

The analytical modelling of the nonlinear Kerr effect is important to analyze nonlinear noise and its impact on the performance of optical transmission systems [1, 2]. Several analytical models have been derived from the nonlinear Schrödinger equation (NLSE). The analytical model that describes nonlinear Kerr effects resulted in a single span system [3] has provided the basis to derive the analytical models of nonlinear wave mixing generated in discretely amplified multi span (lumped) transmission systems [4–6]. The power profile and dispersion accumulation result an oscillation [4–6] (as a function of spectral separation) of the nonlinear products power which was experimentally demonstrated in [7]. The dispersion of the optical fiber has a significant influence on the mixing efficiency where a low dispersion enhances the phase matching bandwidth whilst high dispersion reduces it [8]. In a dispersion managed optical transmission system, dispersion compensating fibers (DCF) can be deployed in a periodic (per span) [9] or in an aperiodic [10, 11] manner and the wave mixing efficiency can be calculated from the coherent summation of fields generated from each fiber in the system [12, 13]. In distributed Raman amplified transmission systems, the more complex signal power variation makes the integration of NLSE hard to solve analytically, so numerical integration (over fiber length) is typically required to describe the nonlinear effects [14], and oscillation in the mixing efficiency is still observed [14].

Mid-link (or multi-) OPC may compensate for some or all of the nonlinear mixing; the level of compensation depends on the symmetry of dispersion and signal power profile in reference to the point of conjugation [15]. The analytical description of the nonlinear mixing

efficiency for a discretely amplified transmission system with mid-link OPC was described in [16] and experimentally verified in [17]. Distributed Raman amplification enhances signal power symmetry and significantly improves the nonlinearity compensation efficiency that the OPC can achieve. Although a mid-link OPC can achieve full inter-signal nonlinearity compensation (with ideal symmetric systems), the benefit will still be limited stochastic effects, such as polarization mode dispersion and parametric noise amplification. In general, the impact of such effects may be minimized by deploying multiple OPCs along the system [18–20]. However, whilst analytical descriptions of nonlinear wave mixing efficiencies, allowing the derivation of nonlinear noise, are available for OPC free systems and for lumped amplifier systems employing a single OPC, there is no such analytical description for the more promising cases of multiple OPC and Raman amplifier based OPC systems.

In this paper, we present a consistent approach to the derivation of nonlinear wave mixing efficiencies for both amplification schemes and as a function of the number of OPCs. For completeness, we review prior analytical descriptions [14, 16, 21] in addition to presenting, for the first time, analytical descriptions of nonlinear wave mixing efficiencies with multiple OPC and of Raman amplifier based OPC systems. We verify the key equations by both simulation and selected experimental results, extending our previous experimental work [17] to include experimental measurements obtained from distributed Raman amplifier based OPC systems. For simplicity, we restrict numerical verifications to 1st order distributed Raman systems. In this paper we analyze optical transmission system that deploy standard single mode fibers (SSMF) since the high dispersion accumulation reduces the nonlinear Kerr efficiency, which makes the dispersion uncompensated SSMF an attractive design choice for long-haul transmission systems. We have also studied per-span fully dispersion compensated system to highlight that such systems enhance the nonlinear Kerr efficiency compared to dispersion uncompensated systems.

## 2. Nonlinear Kerr power in optical transmission systems without OPC

In discretely amplified systems, an optical amplifier (often an erbium doped fiber amplifier EDFA) is located at the end of each span to compensate for fiber attenuation. In a symmetric uniform optical transmission system, all the spans of the system have the same length, all the in-line amplifiers will provide similar gain ( $G = \exp(\alpha L)$ ). Assuming negligible pump depletion, the analytical solution of the inhomogeneous wave equation [3] which describes the evolution of an optical field (spectrally located at  $\omega_F$ ) resulting from the nonlinear wave mixing between three other optical waves ( $q, r, s$  such that  $\omega_F = \omega_q + \omega_r - \omega_s$ ) can be written (for a system with  $N$  spans each of length  $L$ ) as [12]:

$$E_F(NL) = i \frac{\gamma D}{3} E_q(0) E_r(0) E_s^*(0) e^{(i\delta\beta_F NL)} \left[ \frac{e^{(-\alpha + i\Delta\beta)L} - 1}{-\alpha + i\Delta\beta} \right] \sum_{n=1}^N e^{(i(n-1)\delta\Delta\beta L)} \quad (1)$$

where  $E_k(z)$  is the optical field spectrally located at  $\omega_k$  measured at distance  $z$ ,  $\gamma$  is the effective nonlinear coefficient of a fiber with random birefringence [22], and  $D$  the degeneracy factor arising from mathematically identical permutations of the fields. The commonly known effects of self-phase modulation (SPM), cross phase modulation (XPM), and four wave mixing (FWM) [8] correspond to  $D$  takes values of 1, 3, or 6, respectively, and certain specific ordering of the field components (for XPM). SPM corresponds to the case where a single optical wave is involved in the generation of the nonlinear component ( $\omega_q = \omega_r = \omega_s$ , which takes  $D = 1$ ). XPM and degenerate FWM are often addressed to the same phenomenon where two of mixing components have the same frequency ( $\omega_q = \omega_r \neq \omega_s$ , which takes  $D = 3$ ), non-degenerate FWM (or simply FWM) corresponds to all remaining cases including that of unique optical tones are involved in the nonlinear mixing process ( $\omega_q \neq \omega_r \neq \omega_s$ , which takes  $D = 6$ ). For a dispersion managed system with negligible nonlinearity in the

dispersion compensating modules,  $\delta$  is the ratio of the residual dispersion to fiber dispersion per span [23], and  $\Delta\beta = \beta_q + \beta_r - \beta_s - \beta_F$  is the phase matching coefficient of the fiber which, assuming negligible higher order dispersion, relates to the dispersion factor  $\beta''$  as follows [8]:

$$\Delta\beta = -4\pi^2 \beta'' (f_q - f_s)(f_r - f_s) \quad (2)$$

The terms up to and including the squared bracket in Eq. (1) represents the solution for a single span [3], while the last term represents the phase shift resulted by the accumulation of dispersion along the prior  $N-1$  spans. The total power of the nonlinear product  $|E_F(NL)|^2$  can be written as [5–7]:

$$P_F(NL) = \frac{D^2 \gamma^2}{9} P_q P_r P_s \left[ \frac{\alpha^2 L_{eff}^2}{\alpha^2 + \Delta\beta^2} \right] \left[ 1 + \frac{4e^{(-\alpha L)} \sin^2(\Delta\beta L / 2)}{(1 - e^{(-\alpha L)})^2} \right] \frac{\sin^2(N\delta\Delta\beta L / 2)}{\sin^2(\delta\Delta\beta L / 2)} \quad (3)$$

where  $P_{q,r,s}$  is the total power [summed both polarizations  $|E_x|^2 + |E_y|^2$ , Eq. (21) of [3] and Eq. (55) of [22]] of the mixing waves  $q$ ,  $r$ , and  $s$  launched into the fiber, and  $L_{eff}$  is the effective fiber length ( $L_{eff} = [1 - \exp(-\alpha L)] / \alpha$ ). Equation (3) shows that the power of the mixing product scales quadratically with the nonlinear factor of the fiber ( $\gamma$ ), and cubically with the power per wave (if all waves have the same power). The first two squared brackets in Eq. (3) show that the nonlinear product depends on the fiber properties [3, 8]. The last term governs the impact of inter span quasi-phase matching [4–7] which is maximized when the nonlinear products for each span all add constructively. Figure 1(a) shows the simulation (conducted in VPITransmissionMaker 9.8) and experimental setup to obtain the nonlinear product power generated by the end of the transmission system. The setup uses two tunable CW lasers combined using a 3dB coupler and launched into the transmission system. At the output of the system, the optical spectrum was observed to measure the nonlinear product power ( $P_F$ ) as the separation between the two CW lasers was changed [red arrows on the spectrum of Fig. 1(a)].

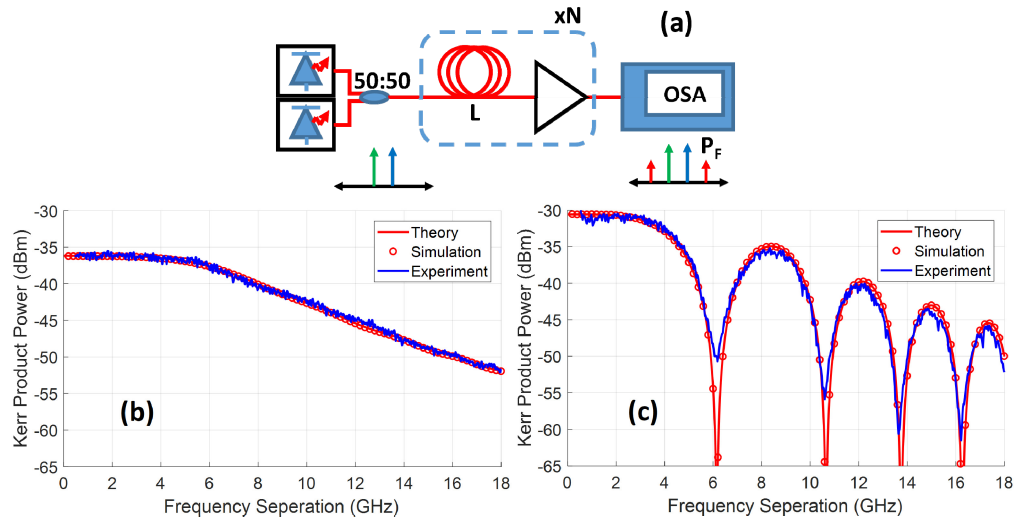


Fig. 1. (a) Simulation and experimental setup, (b) and (c) show the nonlinear Kerr product power as a function of the frequency separation between two CW lasers (0dBm each) for single span, two spans, respectively. Fiber type: G.652,  $L = 100\text{km}$ ,  $\alpha = 0.2\text{dB/km}$ ,  $D_c = 16.4\text{ps/nm/km}$ ,  $\gamma = 1.33\text{km/W}$ .

The figure also shows the power of the nonlinear product as a function of frequency separation between two continuous wave (CW) lasers (0dBm each) propagating through (b) 1x100km and (c) 2x100km dispersion unmanaged ( $\delta = 100\%$ ) EDFA amplified systems. The

EDFAs in the simulation model were noiseless amplifiers (to be able to measure XPM that has low power). The nonlinear product was measured experimentally using a 150MHz resolution optical spectrum analyzer (OSA). The frequency sweeping range throughout this paper does not extend beyond 40GHz, we have chosen this range to avoid the XPM power from falling below the ASE noise level in the experimental validations. As seen from Fig. 1(b), the XPM power degrades quartically as a function of the frequency separation (when  $\Delta\beta \gg \alpha$ ) which can be concluded from Eq. (3). The same quartic degradation can be observed (at the peaks of the XPM power) in the two-span system [Fig. 1(c)]. In general, the main characteristics are as expected [4] and the simulation results show a good agreement with the analytical predictions, while the experimental results show a margin of error of 0.5dB (at the peaks) compared to the analytical predictions. We believe that the mismatching between the analytical predictions and the experimental results at the nulls are due to the limited resolution of the OSA in the experimental setup.

In distributed Raman transmission systems, the power evolution is significantly more complex than the simple propagation loss of a lumped amplifier system [see equation Eq. (2).1.14] in [24] for first order bi-directional pumping], which is in the general case non-integrable. If we divide each distributed Raman span into  $M$  sections over which one may consider the gain or loss coefficient constant, the nonlinear product power can be written as:

$$P_F(NL) = \frac{D^2 \gamma^2}{9} P_q P_r P_s \left[ \sum_{k=1}^M \left[ \frac{e^{(g_k + i\Delta\beta)L_k} - 1}{g_k + i\Delta\beta} \right] \left[ \prod_{l=1}^{k-1} e^{(g_l + i\Delta\beta)L_l} \right] \right]^2 \frac{\sin^2(N\Delta\beta L / 2)}{\sin^2(\Delta\beta L / 2)} \quad (4)$$

where  $L_k$  is the length of the  $k^{\text{th}}$  fiber section (within the span), and  $g_k$  represents the exponential gain/loss constant of the  $k^{\text{th}}$  section. Equation (4) represents a discretized version of the continuous integral reported in [12]. We can see that the last term in Eq. (4) remains unchanged [compared to Eq. (3)], representing quasi-phase matching from span to span, whilst the terms inside  $|\cdot|^2$  represent the solution NLSE over each distributed Raman span. The accuracy of Eq. (4) clearly relies on the number of sections per span ( $M$ ), however, an optimized two-section approximation ( $L_1 \neq L_2$ ) can provide a good approximation for distributed Raman amplification using dominantly forward or dominantly backward pumping schemes [21].  $M$  should be selected based on the desired accuracy and the number of pumps, since firstly the number of sections where the signal power is either increasing or decreasing increases in proportion to the number of pumps and secondly the curvature of these individual sections is more accurately modelled with a larger number of sections rather than an aggregate gain/loss value. In our non-exhaustive experience 4 times the number of pumps gives a reasonable approximation, and 32 equally spaced sections would be a practical upper limit. Figure 2 shows validation of Eq. (4) by simulation for a first order Raman pumped span, Fig. 2(a) shows the XPM power as a function of frequency separation (between two CW lasers), Fig. 2(b) shows the power profile along the 62-km span. The validation considered different ratios of forward to backwards pump power ( $r_f = P_{fw}/(P_{fw} + P_{bw})$ ) subject to a condition of zero net loss. The theoretical solutions were obtained using 31-sections with  $g_i$  calculated for Fig. 2(a). At low frequency separation ( $\Delta\beta \rightarrow 0$ ), the power of the nonlinear product increases with an increasing fraction of forward pumping ( $r_f$ ), due to the increase in peak signal power along the span.

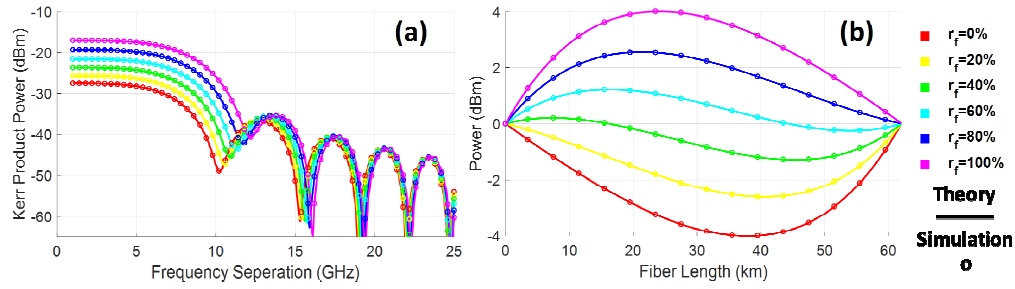


Fig. 2. (a) Nonlinear Kerr product power as a function of frequency separation between two CW lasers (0dBm each) propagating through 1st order Raman pumped 62km span, (b) corresponding power profiles for each  $r_f$ . Fiber type: G.652.

Figure 2(a) show that the occurrence of the first null in XPM power shifts to higher frequency separation as  $r_f$  moves from 0% to 100%, the simulation results show a good agreement with the theoretical predictions. For higher frequency spacing, oscillation is observed due to the intra span phase matching described by summation in Eq. (4). For sufficiently high frequency separation (beyond 20GHz in this case), the phase mismatching dominates over gain/loss ( $\Delta\beta \gg g_x$ ) and the nonlinear wave mixing power converges to (regardless of pumping scheme):

$$P_F(NL) = \frac{D^2 \gamma^2}{9} P_q P_r P_s \frac{4 \sin^2(N \Delta \beta L / 2)}{\Delta \beta^2} \quad (5)$$

The convergence towards fixed null positions for frequency separation beyond 20 GHz may be clearly observed in Fig. 2(a). Figure 3 shows validation of Eq. (4) by experiment for a second order Raman pumped span [25], Fig. 3(a) shows the XPM power as a function of frequency separation (between two CW lasers), Fig. 3(b) figure shows the normalized power profile along the 62-km span. The experimental validation considered different  $r_f$  (as shown in the legend), and the theoretical solutions of XPM were obtained using 31-sections with  $g_i$  calculated from optical time domain reflectometer (OTDR) measurements for Fig. 3(b). The CW laser power was changed by a factor of 0.4dB for each  $r_f$  step, which correspond to achieve the same experimental nonlinear product power at low frequency separation. The CW laser power used for Fig. 3 was varied to maintain constant efficiency at low spacing to emphasize nonlinear power variations (at higher frequency spacing) and the location of the first null occurrence (for different power profiles). The experimental results show good agreement [within 0.7dB margin of error at the peaks, Fig. 3(b)] with the theoretical predictions; the mismatch in the null depth between the experimental and theoretical results occurs due to the limited resolution of the OSA. We note that Eq. (5) is also valid for ideal lossless Raman amplification, which experiences the same limit of Eq. (4) as  $g_x \rightarrow 0$ .

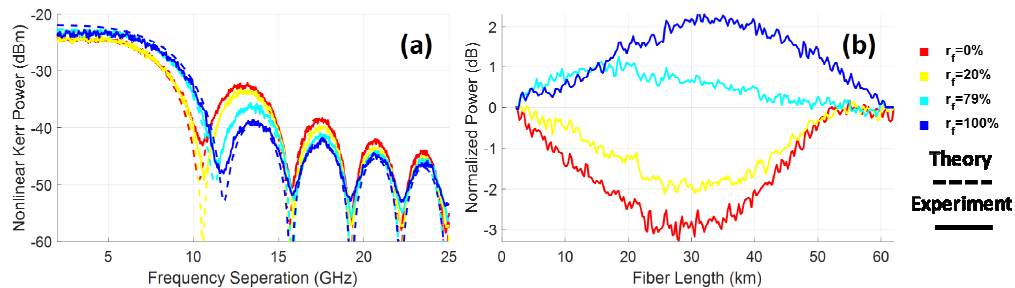


Fig. 3. (a) Nonlinear Kerr product power as a function of frequency separation between two CW lasers (0.5dBm, 0.1dBm, -0.3dBm, and -0.6dBm each for  $r_f = 0\%$ , 20%, 79%, and 100%, respectively) propagating through 2nd order Raman pumped 62km span and (b) shows the corresponding power profiles [21]. Fiber type: G.652.

### 3. Nonlinear Kerr power in OPC-assisted optical transmission systems

We next consider the net nonlinear wave mixing efficiency for the general case of multiple OPCs. As shown in Fig. 4, there are two common approaches reported to deploy OPCs along a link with regularly spaced amplification: single segment spaced OPCs where the number of spans between signal processing elements (transmitters, OPCs and receivers) are equal [18–20], as is the case for mid-link OPC, and double segment spaced OPCs where the number of spans between the transmitter/receiver and the nearest OPC is half the number of spans between two consecutive OPCs [26]. For notational convenience we consider that the number of segments with single segment spaced OPCs is  $N_{seg} = N/(N_{OPC} + 1)$ , whilst the number of for double segment spacing is:  $N_{seg} = N/(2N_{OPC})$ .

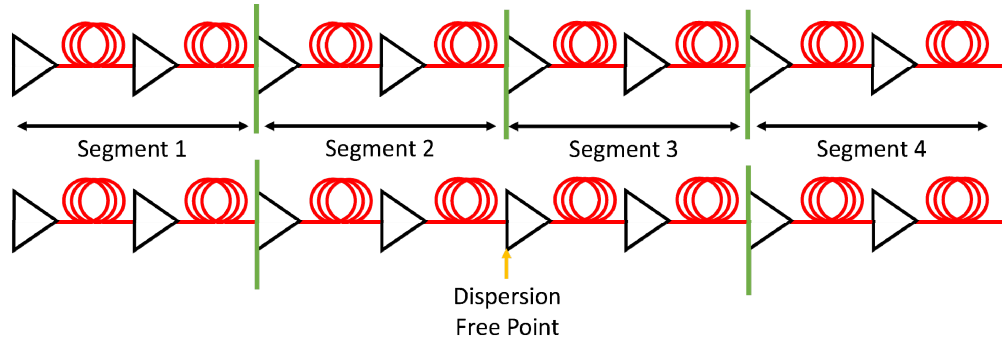


Fig. 4. OPC deployment techniques. (top) single segment spaced OPCs, (bottom) double segment spaced OPCs.

An even number of segments is most interesting as it offers the prospect cancellation of the nonlinear wave mixing and corresponds to an odd number of OPCs in a single segment configuration, or an even number in a double segment configuration. Given that after any two consecutive segments all dispersion effects are compensated (neglecting higher order dispersion), all pairs of segments generate the same nonlinear field; so, the total field amplitude  $E_F$  of the nonlinear product is:

$$E_F(NL) = \frac{N_{seg}}{2} \left[ E_F(\text{even segment}) + [E_F(\text{odd segment})]^* e^{i\delta\beta_F NL/N_{seg}} \right] \quad (6)$$

The terms in the squared brackets [of Eq. (6)] represent the coherent summation of the nonlinear field resulting from any two consecutive segments in the link. For discretely amplified transmission systems, the accumulated nonlinear field from an odd indexed segment (with  $N/N_{seg}$  spans) can be written as [as Eq. (1) but with  $N$  replaced by  $N/N_{seg}$ ]:

$$E_F(\text{odd segment}) = i \frac{\gamma D}{3} E_q(0) E_r(0) E_s^*(0) e^{i\delta\beta_F NL/N_{seg}} \left[ \frac{e^{([- \alpha + i\Delta\beta]L)} - 1}{-\alpha + i\Delta\beta} \right] \sum_{n=1}^{N/N_{seg}} e^{i(n-1)\delta\Delta\beta L} \quad (7)$$

By the end of the odd indexed segment, the mixing fields ( $q$ ,  $r$ , and  $s$ ) are phase shifted according to the accumulation of dispersion along the segment ( $\exp(i\delta[\Delta\beta + \beta_F]NL/N_{seg})$ ). Then these fields are conjugated to propagate through the following even indexed segment of the link which results the following nonlinear field:

$$E_F(\text{even segment}) = i \frac{\gamma D}{3} E_q^*(0) E_r^*(0) E_s(0) e^{-i\delta\Delta\beta L} \left[ \frac{e^{([- \alpha + i\Delta\beta]L)} - 1}{-\alpha + i\Delta\beta} \right] \sum_{n=1}^{N/N_{seg}} e^{-i(n-1)\delta\Delta\beta L} \quad (8)$$

Substituting Eq. (7) and Eq. (8) into Eq. (6) gives the total nonlinear field generated by the OPC system which can be written as:

$$E_F(NL) = i \frac{\gamma D N_{seg}}{6} E_q^*(0) E_r^*(0) E_s(0) \left[ e^{(-i\delta\beta L)} \frac{e^{[-\alpha+i\Delta\beta]L} - 1}{-\alpha + i\Delta\beta} - \frac{e^{[-\alpha-i\Delta\beta]L} - 1}{-\alpha - i\Delta\beta} \right] \sum_{n=1}^{N/N_{seg}} e^{(-i(n-1)\delta\beta L)} \quad (9)$$

or in terms of power as:

$$P_F(NL) = \frac{D^2 \gamma^2 N_{seg}^2}{36} P_q P_r P_s \left| e^{(-i\delta\beta L)} \frac{e^{[-\alpha+i\Delta\beta]L} - 1}{-\alpha + i\Delta\beta} - \frac{e^{[-\alpha-i\Delta\beta]L} - 1}{-\alpha - i\Delta\beta} \right|^2 \frac{\sin^2(N\delta\beta L / [2N_{seg}])}{\sin^2(\delta\beta L / 2)} \quad (10)$$

Equation (10) can be simplified for fully dispersion compensated system ( $\delta = 0$ ) as:

$$P_F(NL) = \frac{D^2 \gamma^2}{9} \frac{P_q P_r P_s N^2}{(\alpha^2 + \Delta\beta^2)^2} \left[ \alpha e^{-\alpha L} \sin(\Delta\beta L) + \Delta\beta (e^{-\alpha L} \cos(\Delta\beta L) - 1) \right]^2 \quad (11)$$

and for dispersion uncompensated system ( $\delta = 1$ ) as:

$$P_F(NL) = \frac{D^2 \gamma^2 N_{seg}^2}{9} \frac{P_q P_r P_s}{(\alpha^2 + \Delta\beta^2)^2} \left[ \alpha (e^{-\alpha L} + 1) \sin\left(\frac{\Delta\beta L}{2}\right) + \Delta\beta (e^{-\alpha L} - 1) \cos\left(\frac{\Delta\beta L}{2}\right) \right]^2 \frac{\sin^2(N\delta\beta L / [2N_{seg}])}{\sin^2(\delta\beta L / 2)} \quad (12)$$

Equation (11) shows that the fully dispersion compensated discretely amplified system with mid-link OPC has the same wave mixing efficiency irrespective of the number of OPCs, as the full dispersion compensation ensures all spans add coherently with identical phase. For the dispersion uncompensated case, the frequency spacing between quasi-phase matching peaks is strongly dependent on the number of segments. The square bracketed terms in Eq. (11) and Eq. (12) show that an OPC-assisted discretely amplified system rarely provides *full* nonlinearity compensation. A full nonlinearity compensation ( $P_F(NL) = 0$ ) can be realized in dispersion uncompensated systems when either deploying a full link of dispersion-less optical fiber ( $\beta'' = 0$ ), or deploying lossless spans ( $\alpha = 0$ ). The two conditions ( $\beta'' = 0$  and  $\alpha = 0$ ) must be present to achieve full nonlinearity compensation in fully dispersion managed system. A pre-OPC dispersion compensating stage have been proposed and experimentally validated by [27, 28] to minimize the nonlinear Kerr effects resulted in OPC assisted discretely amplified system, such system can be analytically modelled by scaling the second term in the squared brackets of Eq. (9) by  $\exp(i\Delta\beta_{DC}L_{DC})$ ; where  $\Delta\beta_{DC}$  and  $L_{DC}$  represent the phase mismatching and the length of the dispersion compensating module used before the OPC. This technique provides an optimization factor that can minimize the asymmetric placement of the OPC, but does not show full nonlinearity compensation as concluded in [27]. Other asymmetric OPC deployment (non-mid-link) have been suggested in [29], these systems can also be analytically modelled by altering the upper bound of the summations in Eq. (6) and (7). In this paper, we will analyze the symmetric systems for their analytical simplicity.

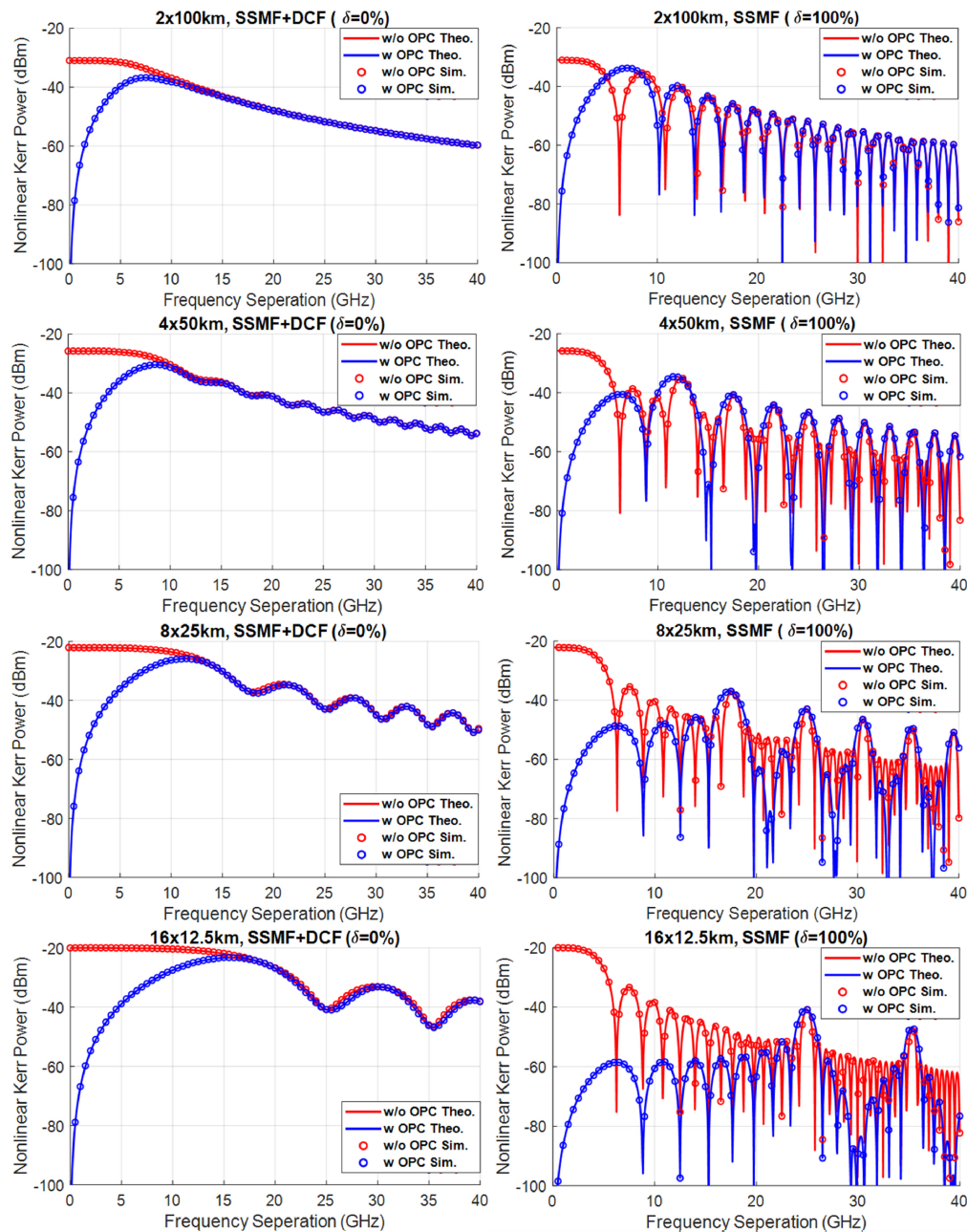


Fig. 5. Nonlinear Kerr product power as a function of frequency separation between two CW lasers (0dBm each) propagating through 200km lumped transmission system (with different span length). (left column) fully dispersion compensated system with 0% residual dispersion, (right column) dispersion uncompensated system. Fiber type: G.652.

Figure 5 compares the theoretical predictions with numerical simulations with (left) and without (right) dispersion management for a 200km discretely amplified system for a range of span lengths assuming two CW lasers are input to the system with launch powers of 0dBm. The results are shown for a link without mid-link OPC [red, Eq. (3)] and a link with ideal mid-link OPC [blue, Eq. (11) and Eq. (12)]. The optical fiber parameters used in the simulations were the same as described in the caption of Fig. 1. Excellent agreement with

simulations and numerical simulations is observed in all cases confirming the accuracy of the analytical predictions. With full dispersion compensation ( $\delta = 0\%$ ), the power of the nonlinear mixing product without mid-link OPC scales with  $(NL_{eff})^2$  which results in increasing nonlinear mixing product with reducing span length. In this analysis, we have kept the CW laser power to 0dBm to point out the increments of XPM power as the span length gets shorter and observe that the nonlinear power scales by  $(NL_{eff})^2$ . In designing systems with different span lengths, one might consider that a reduction of launched CW power (by  $(NL_{eff})^{2/3}$ ) into the fiber as the span length gets shorter to be a good design strategy. Quasi phase matching is not observed as predicted by the last term of Eq. (3), equal to  $N^2$  for  $\delta = 0$ . The observed frequency spacing dependent oscillations, which grow in amplitude with reducing span length correspond to intra-span phase matching [second squared bracket in Eq. (3)] and have a magnitude which scales with the span loss. With mid-link OPC and full dispersion compensation gives a strong reduction in net nonlinear wave mixing for narrow frequency spacing (corresponding to strong phase matching). The reduction in nonlinear wave mixing efficiency starts to fade away as the frequency spacing increases until there is no compensation (corresponding to weak phase matching). This lack of compensation that the OPC can achieve in fully dispersion compensated systems can be theoretically concluded from Eq. (11) as the second term in the squared brackets dominates the nonlinear product power in the weakly phase matched region ( $\Delta\beta \gg \alpha$ ) and this term is identical to the corresponding term for a system without OPC [Eq. (3)].

Intuitively, one obtains the best compensation when  $\alpha$  and  $\Delta\beta$  are small because the nonlinear products generated before and after the OPC may easily be phase aligned for ideal cancellation. But for high beta, rapid evolution of the phase of the mixing products makes this increasingly difficult to achieve cancellation for all frequency separations simultaneously [as shown by the rapid oscillations in Fig. 5 (right column)]. The bandwidth over which nonlinearity compensation occurs in a fully dispersion compensated transmission system grows slowly as the span length decreases (10GHz for 2x100km system to 17GHz for 16x12.5km system) suggesting that only intra-channel nonlinear effects may be compensated for using an OPC, albeit all channels being compensated simultaneously in a single device.

In dispersion uncompensated system without OPC [Fig. 5, right column], the nonlinear mixing efficiency in the strongly phase matched regime also scales as  $(NL_{eff})^2$  and matches the nonlinear mixing efficiency for a fully dispersion compensated system at the quasi phase matching peaks ( $\Delta\beta L = 2 m \pi$ ). With a mid-link OPC a strong reduction in the net nonlinear mixing efficiency is always observed in the strongly phase matched regime. For a system with a long span length and only one span per segment (2x100km) the net wave mixing efficiencies converge at higher frequency separation and no net compensation occurs in the weakly phase matched regime. This may be seen from Eq. (3) and Eq. (12) in the limit ( $e^{-\alpha L} \rightarrow 0$ ) where the different combinations of intra and inter span phase matching converge for large  $\Delta\beta L$  and the quasi phase matching peaks coincide. As the number of spans increase however, the number of nulls between quasi-phase matching peaks is almost halved. For high span loss ( $\alpha L > 0.5$ ), there is no net reduction in nonlinear mixing efficiency at the quasi-phase matching peaks, and the peaks themselves are doubled in width, although a degree of nonlinearity compensation occurs between the peaks. Reducing the span length enhances the extent to which this compensation occurs. For low span loss (not shown as we view sufficiently low span loss to be commercially impractical), substantial reduction in the net nonlinear wave mixing efficiency is possible even at the quasi-phase matching peaks.

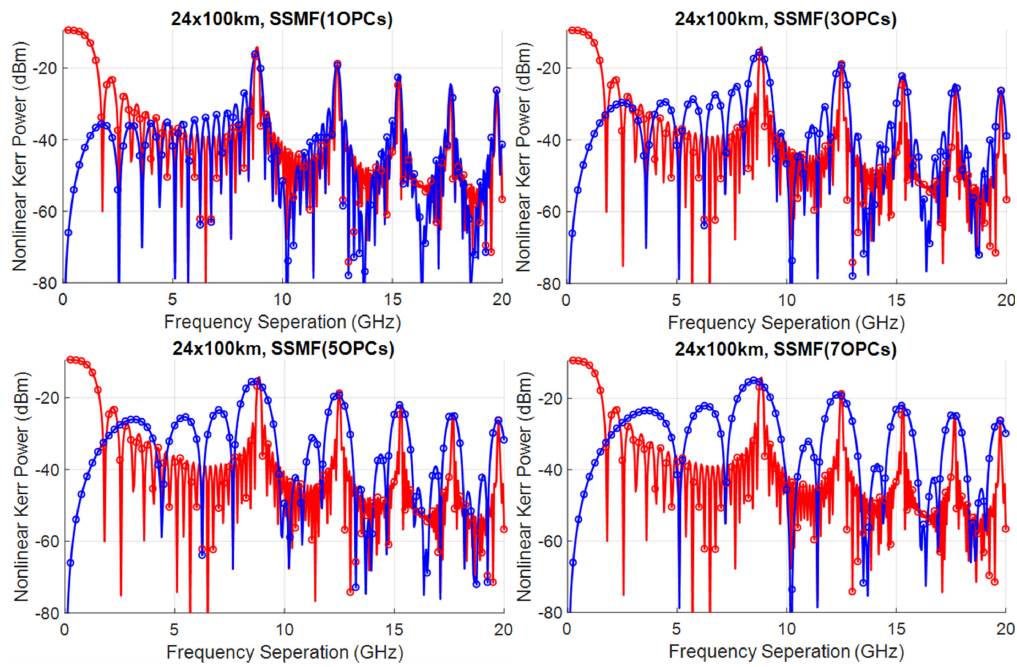


Fig. 6. Nonlinear Kerr product power as a function of frequency separation between two CW lasers (0dBm each) propagating through 24x100km lumped transmission system with different number of equally spaced and symmetrically located OPCs (1OPC, 3OPCs, 5OPCs, and 7OPCs). (red) without OPC, (blue) with OPCs, (solid lines) theory, (open circles) simulation results. Fiber type: G.652.

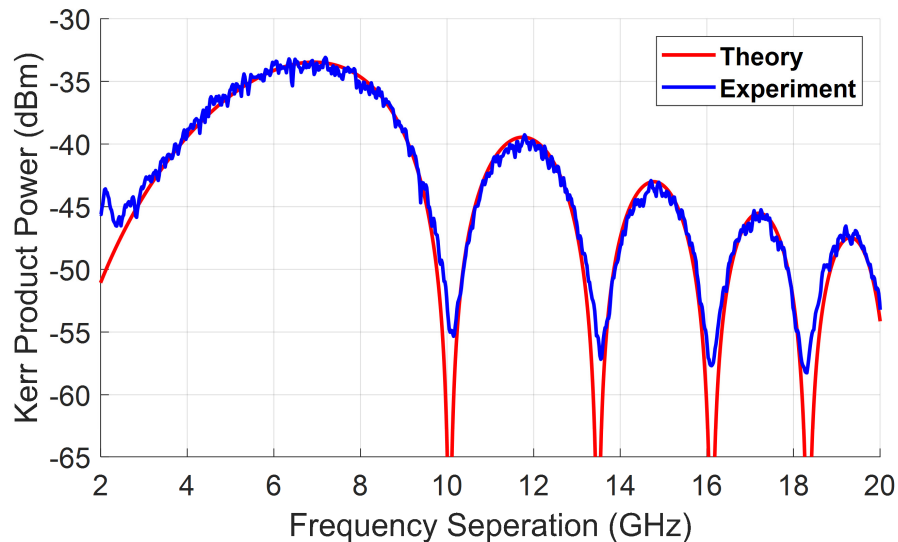


Fig. 7. Nonlinear Kerr power as a function between two CW lasers passing through 2x100km transmission system with a mid-link OPC [17]. Fiber type: G.652.

Figure 6 shows the power of the nonlinear wave mixing product as a function of the frequency separation between two CW lasers transmitted over a 24x100km discretely amplified system with different numbers of OPCs, and once more shows excellent agreement

between analytical predictions and numerical simulations. The zero OPC case is plotted in all panels to aid comparison. The figure shows that the introduction of OPC still results compensation in the strong phase matching regime. As the span loss is high, negligible compensation occurs at the quasi-phase matching peaks, and increasing the number of OPCs increases the width of each peak and so diminishes the nonlinearity compensation. In the extreme case of one OPC per span ( $N_{seg} = N$ ) the system behaves as a fully dispersion compensated system with a single OPC [Eq. (11)] and the total mixing efficiency is higher with an OPC every span than without any. Figure 7 shows an experimental validation of Eq. (12), the figure shows the power of the nonlinear mixing product power as a function of frequency separation between two CW laser propagating through a 2x100km system with an OPC in between the two spans. The setup uses three EDFAs: one to compensate for the loss of the first span, one to compensate for the OPC loss, and one to compensate for the loss of the second span. We used a dual pump polarization insensitive OPC, the two OPC pumps were counter dithered by two tones (60MHz and 600MHz) to increase SBS threshold as described fully in [17]. The experimental results show a good agreement with the theoretical predictions within a margin of error of less than 0.5dB (at the peaks), and a mismatching at the nulls due to the limited OSA resolution.

In distributed Raman transmission system, the power of the nonlinear mixing products of a link including one or more OPCs may be calculated by substituting on Eq. (4) into the derivation [Eq. (6) to Eq. (10)] instead of Eq. (3); which gives:

$$P_F(NL) = \frac{D^2 \gamma^2 N_{seg}^2}{9} P_q P_r P_s \frac{\sin^2(N\Delta\beta L / [2N_{seg}])}{\sin^2(\Delta\beta L / 2)} \left[ e^{(-i\Delta\beta L)} \sum_{k=1}^M \left[ \frac{e^{(g_k + i\Delta\beta)L_k} - 1}{g_k + i\Delta\beta} \right] \left[ \prod_{l=1}^{k-1} e^{(g_l + i\Delta\beta)L_l} \right] - \sum_{k=1}^M \left[ \frac{e^{(g_k - i\Delta\beta)L_k} - 1}{g_k - i\Delta\beta} \right] \left[ \prod_{l=1}^{k-1} e^{(g_l - i\Delta\beta)L_l} \right] \right]^2 \quad (13)$$

The equation still shows [as Eq. (10)] quasi-phase matching within each segment and coherent addition of nonlinear mixing fields from odd and even numbered segments (last term). Figure 8 (right column) shows the nonlinear mixing product power resulted from the propagation of two CW lasers a through 200km distributed Raman system with pump intervals, the power profile per span is shown in the left column. Longer pump intervals will have larger signal power excursions and larger variability with pump configuration. As a result, power of the mixing product in the strongly phase matched regime is higher for span length. Once more, the use of an OPC significantly reduces the nonlinear mixing product in the strongly phase matched region regardless of the span length or the pumping scheme. For intermediate phase matching, the nonlinearity compensation is reduced, especially for systems with long span length (100km) reaching its maximum value at frequency separation ranging around 8GHz (for 2x100km system), 12GHz (for 4x50km system), 17GHz (for 8x25km), and 25GHz (for 16x12.5GHz). Beyond these frequencies, the nonlinear mixing efficiency is dominated by the propagation constant difference. In general, as the frequency separation raise above the frequency separation at which the nonlinear product power reached its maximum (in OPC assisted system), the nonlinear product power starts to decline at higher rate compared to the one resulted in a system without OPC; the reasoning for that is the fact the value of  $\Delta\beta$  starts to dominate over gain/attenuation coefficients ( $g_x$ ) which gets the system to get closer to the OPC assisted quasi-lossless Raman system that provide full compensation of the nonlinear Kerr effects.

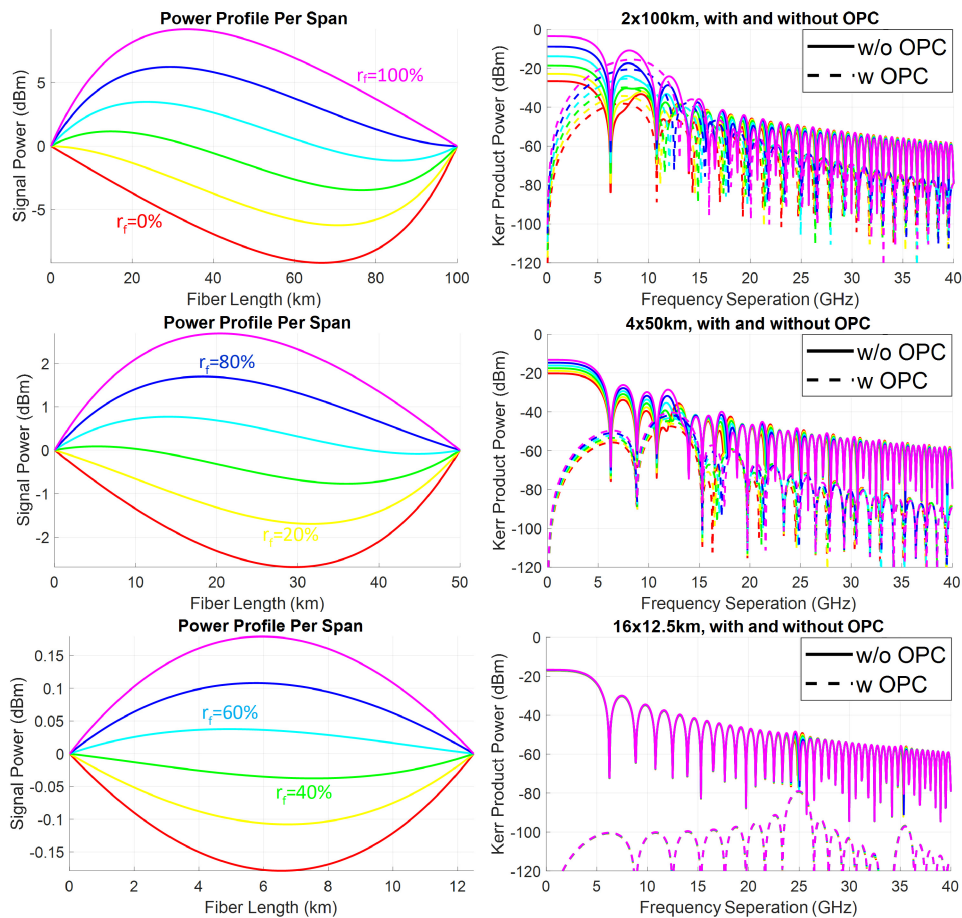


Fig. 8. (left column) the power profiles of distributed Raman ranging from  $r_f = 0\%$  to  $100\%$  with a step of  $20\%$ . (right column) Nonlinear Kerr product power as a function of frequency separation between two CW lasers ( $0\text{dBm}$  each) propagating through  $200\text{km}$  first order distributed Raman transmission system (with different span length). (solid lines) without mid-link OPC, (dashed lines) with mid-link OPC, the color code represents the different power profiles displayed on the left side. Fiber type: G.652.

Unlike a lumped amplification system, in all cases the OPC provides a significant reduction in the net nonlinear mixing efficiency when Raman amplification is employed, even if in certain circumstances (for example a frequency spacing of  $6\text{GHz}$  in a  $100\text{km}$  span system) the net efficiency remains high. This is especially true at shorter span lengths where over a  $25\text{dB}$  suppression is observed in the Raman system with  $12.5\text{km}$  spans, whilst negligible suppression is observed in an equivalent lumped system at the quasi phase matching peaks with a maximum suppression below  $20\text{dB}$  elsewhere. This broadband suppression of nonlinear mixing efficiency when Raman amplification and OPC are combined is particularly attractive in the context of a fully loaded WDM system. Figure 9 shows a validation of the analytical predictions [Eq. (13)] against numerical simulations results for a  $24 \times 50\text{km}$  distributed Raman system [with the six power profiles of Fig. 8(b)] with different numbers of OPCs. Again, the theoretical predictions match the simulation results. The results still show that the multi-OPC solution in distributed Raman systems causes a broadening in the peaks in nonlinear mixing efficiency corresponding to quasi-phase matching. In terms of the inter-signal nonlinearity considered here, this broadening will result a degradation in the compensation efficiency as the number of OPCs is increased. However,

given that over 25dB compensation is possible the system is likely to be limited by stochastic effects such as PMD, reducing the compensation efficiency, and parametric noise amplification, both show monotonic improvement as the number of OPCs is increased, suggesting that an optimum number of OPCs will exist for Raman amplified OPC based links.

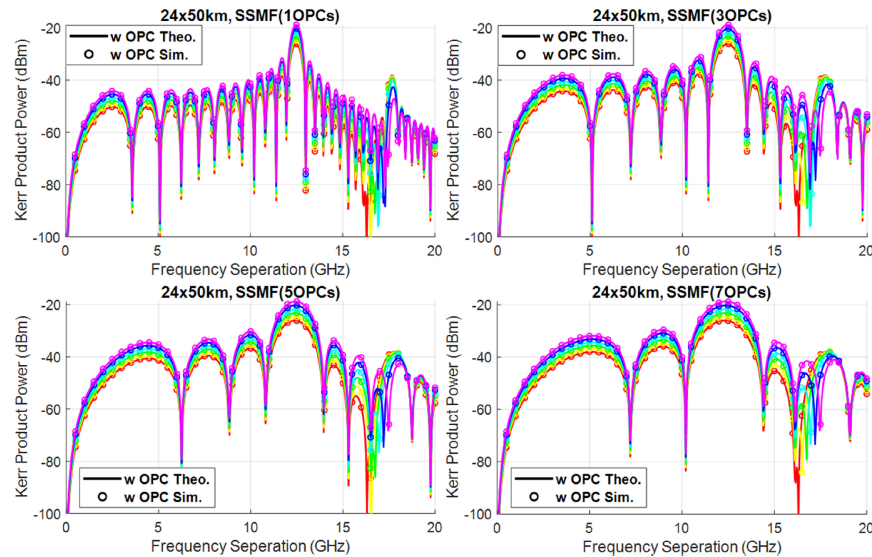


Fig. 9. Nonlinear Kerr product power as a function of frequency separation between two CW lasers (0dBm each) propagating through 24x50km distributed Raman transmission system with different number of equally spaced and symmetrically located OPCs (1OPC, 3OPCs, 5OPCs, and 7OPCs). (solid lines) theory, (open circles) simulation results, colors represent different  $r_f$  values, same color code as Fig. 8. Fiber type: G.652.

To experimentally validate Eq. (13), we built a 2x50km distributed Raman transmission system and evaluated the nonlinear mixing products generated by two CW lasers (6dBm each), as shown in Fig. 10. A high-power Raman pump (located at 1455nm) was split equally to be injected (using a wavelength division multiplexer) in the backward direction of the two 50km spans. An isolator was used to prevent any remains of the Raman pump to pass through to the lasers or EDFAs. In between the two spans two paths were created: with and without OPC. In both paths an EDFA is used to restore the laser powers to 6dBm. The path with the OPC used an EDFA pre-amplifier, band pass filters to eliminate out of band ASE noise, a single fiber grating filtered high-power pump, and a highly nonlinear fiber ( $L = 170\text{m}$ ,  $\lambda_0 = 1549.7\text{nm}$ ,  $\gamma = 14/\text{W/km}$ ). OTDR measurements of power profile [shown as an inset to Fig. 10] were performed on both spans and compared with the theoretical power profile showing a good agreement. Figure 11 illustrates a close match between the experimental results and analytical predictions with 0.8dB margin of error and confirm significant nonlinearity compensation over the full bandwidth of the measurement (except at the nulls). The mismatch with the theoretical predictions at the nulls is due to the amplified spontaneous emission (ASE) noise floor induced by the inline EDFAs.

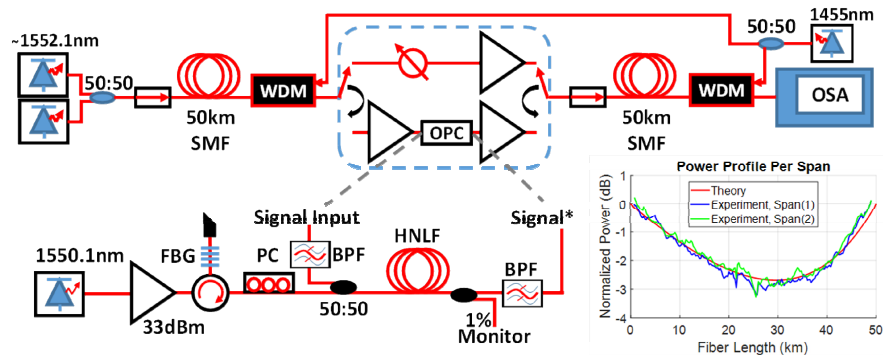


Fig. 10. 2x50km backward pumped 1st order distributed Raman transmission system (with and without mid-link OPC) passing through two CW lasers (with varying frequency separation). Each CW propagating through the system enter the Raman span with 6dBm power, Raman pump (1455nm) power was calibrated to achieve 0dB net gain. The inset figure on the bottom right shows the OTDR measurements of the power profile along the 1st order distributed Raman amplified 50km spans compared with the theory [as reported in Fig. 8].

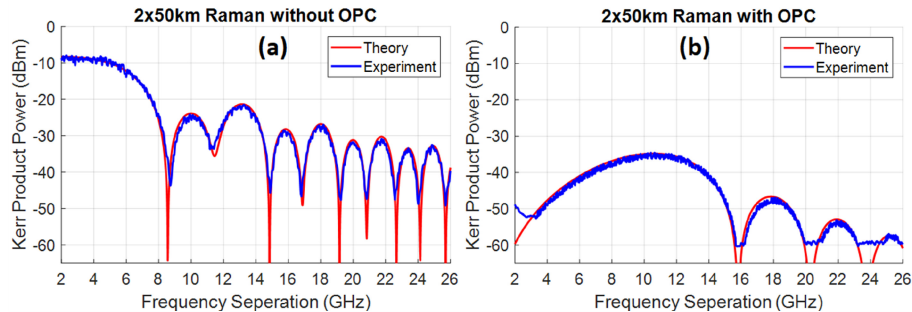


Fig. 11. The nonlinear Kerr power as a function between two CW lasers passing through 2x50km backward pumped 1st order distributed Raman transmission system without OPC (a) with mid-link OPC (b).

## Conclusions

We have presented analytical equations describing the nonlinear wave mixing efficiency for periodically amplified optical transmission systems using both lumped and Raman amplifiers, and for an arbitrary number of OPCs, allowing for the inclusion of span-by-span dispersion management. The closed form equations were all verified against numerical simulations, and selected configurations verified experimentally. In addition to a consistent approach, allowing a direct comparison of the various link configurations, we have introduced for the first time generic equations for distributed Raman systems with arbitrary number of OPCs. Our verification results show that nonlinearity compensation efficiency is always high in the strongly phase matched regime, and improves as the signal power within a span reduces, either through Raman amplification, or via reduced span length. An OPC-assisted distributed Raman amplified systems always provide a higher compensation efficiency compared to an equivalent OPC-assisted discretely amplified system, and retains its efficiency over the full range of frequency separations studied. However, in contrast to stochastic effects, such as signal noise interactions, which favor a multi-OPC configuration, we have seen that the multi-OPC approach always diminishes the level of nonlinearity compensation for inter signal effects compared to a single OPC, suggesting that an optimum number of OPCs exists. Finally, we would note that whilst dispersion compensated OPCs [29] are not considered explicitly here, we anticipate that the general trends observed here will remain valid. The closed form equations presented in this work provide the basis to the calculation of nonlinear

noise generated from spectrally efficient WDM modulated signals, this calculation requires the double integral of the presented equations over the modulated signals bandwidth. As was shown in [2, 22, 23], the total nonlinear noise generated in a WDM system can be derived from Eq. (3) (for discretely amplified transmission systems without OPC).

Original data for this work is available through Aston Research Explorer (<http://doi.org/10.17036/researchdata.aston.ac.uk.00000304>).

### **Funding**

The Engineering and Physical Sciences Research Council (EPSRC) (EP/J017582/1 [UNLOC], EP/L000091/1 [PEACE]), and Marie Curie Initial Training Networks (FP7 ITN) (608099 [ICONE]).